Repeat-pass Autofocus for airborne polarimetric Synthetic Aperture Radar Tomography

J Cantalloube, Alice Combernoux, Héléne Oriot

Repeat-pass Autofocus for airborne polarimetric Synthetic Aperture Radar Tomography.

Hubert M.-J. Cantalloube *, **Alice Combernoux** **, **Hélène Oriot** ***

*ONERA
chemin de la Hunière et des Joncherettes, 91761 Palaiseau-CEDEX, FRANCE
email: cantallo@onera.fr

**ONERA
email: alice.combernoux@onera.fr

***ONERA
email: helene.oriot@onera.fr

Abstract: *Synthetic aperture radar tomography, or volume imaging with a side-looking radar uses a two-dimensional aperture made of several antenna paths along more or less parallel trajectories. The carrier motion providing the along track extension of the aperture, and the across-track extension is provided by multiple cross-track antenna or by repeated acquisition along parallel lines. The relative position of the individual antenna centres within the aperture is highly demanding (its accuracy requirement is in the order of magnitude of on tenth of wavelength). The absolute positioning is less demanding: it has an impact on the image registration (which does not require accuracy beyond the image resolution, typically several wavelengths) and to a lesser extend to the topographic effects in motion compensation (but DTM resolution is generally even much lower than that of the image). The relative successive positions during the aperture can be refined by autofocus (using the resulting image sharpness to increase the trajectory accuracy) for the along-track separation. For the across-track separation, especially in repeat-pass airborne acquisitions, the same direct approach is not feasible because volume extension of the landscape is low (typically the height of a tree compared to the image stripe length) and the aperture sampling across-track is sparse (each new antenna centre require a new acquisition line that takes tens of minutes of flight). Co-registration by correlating the images obtained from individual acquisition lines is not enough since the autofocus only refines the relative positions within the along-track aperture, leaving error build up at low frequency.*

Here we propose and evaluate two solutions: The first one is to separately autofocus the acquisition lines and then recover the low frequency positioning errors between the acquisition lines by measuring the distortion field between the images obtained from each acquisition line and deriving the low frequency relative errors. The second is to autofocus the first (or master) acquisition line and then "refocus" the other acquisition lines using the master signal as reference in a way derived from the bistatic autofocus.

To compare the methods, we use the 18 calibrations passes of a three week long airborne acquisition campaign with two antenna centre, providing full polarimetric measurement on one side and dual polar measurement on the other side (thus providing 36 separate trajectories for the Vv and Hv channels and 18 for the Hh and Vh channels).

978-3-7369-9343-3

1. Introduction

Beyond surface imaging, side looking radar (SAR) has, under certain conditions, the capability of penetrating the vegetation cover (as well as some soils or building covers see fig. 1 for example) thus gaining information useful for remote sensing from biomass estimation, crop assessment, surface moisture measurement or archaeology to military under foliage detection or intelligence.
These remote sensing objective, however, often rely on target modelling and inversion of the model. E. g. the biomass density of an extended forest cover can be estimated from the backscattering level of just two polarisation channels. Tuning and qualifying such a model requires labour intensive (and tedious) ground truth measure that 3D radar imaging (tomography) may alleviate.
Gaining resolution in the third dimension (thickness) requires extending the radar aperture across-track. In SAR, the along-track extension of the aperture is almost always obtained by sensor motion, across-track extension however can be obtained by scanning with a linear antenna array perpendicular to motion (think of landmine detection army scanners or through-the-cloth weapon/explosive scanners at airport security) but for airborne remote sensing, it is difficult to extend the antenna array beyond the aircraft wingspan, hence the aircraft herself should scan a 2D pattern (typically nearly parallel lines filling a rectangular area).

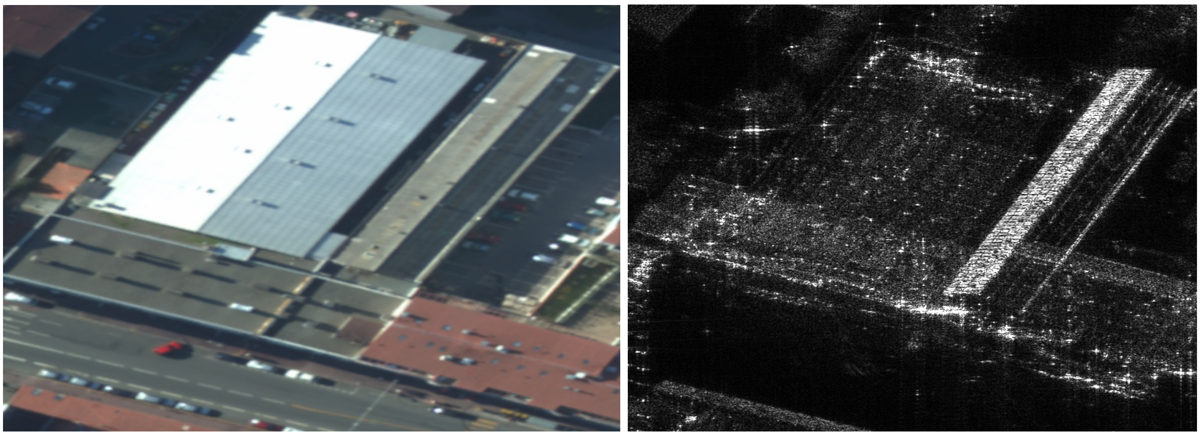

Figure 1: Example of building roof opaque in visible light (left) but transparent at X-band (right). White roofed building hosts a supermarket the aisles of which can be discerned at X-band.

In order to focus the 2D synthetic antenna, the positions of the phase centres involved into the synthetic aperture should be known with an accuracy of typically a tenth of the wavelength (the exact value depends on the tolerance for blur and side lobe). In fact, it is the relative position which is critical since a collective translation or tilt error only result in a localisation error on the resulting image. The point is that the accuracy of aircraft trajectory measure is in the order of 10 cm (it is obtained by inertial measurement hybridised by multilaterating with GNSS signal at L-band). Hence, for smaller wavelength such as widely used C and X bands, the trajectories must be updated from the recorded signal itself.
In fact, for standard (i. e. 2D) SAR imaging, autofocus may not be mandatory due to the fact that accuracy at short term on the trajectory may meet the requirement. For example: the image

of fig. 2 at X-band is integrated (duration of the synthetic aperture) 2.4 s (290 m along track) and its 30 cm resolution is attained without autofocus, however, positioning errors at frequency lower than 0.42 Hz cause significant image distortion of the order of 4 m at a 5 km range (this can be assessed by the position of four visible geodetic landmarks of which the absolute position is known to 4 cm approximately).

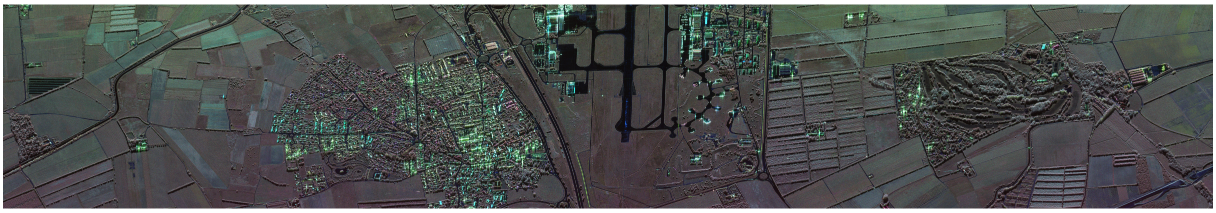

Figure 2: One of the images of the TBA dataset at X-band (flight 2, take 1) processed from raw trajectory, with Vv channel rendered as blue, Hh channel rendered as green and Hv & Vv channels rendered as red. Swath width is 1.2 km (slant), stripe length is 7.13 km. Slant range & azimuth resolutions are both 30 cm.

For the 2D aperture however, autofocus is mandatory since the acquisition lines are separated at best by minutes (the acquisition of fig. 2 is one minute long, a typical aircraft U-turn is also one minute and margins must be granted for alignment after the U-turn.). In our TBA dataset, the 18 successive line acquisitions are separated by up to three weeks and the raw image mismatch is about 4 meter for the worst case to about 70 cm for the most common cases. As a matter of fact, the worst case is that of fig. 2. Typical accuracy without autofocus nor registration to known landmarks at this range is around 70 cm but our IMU was probably not functioning perfectly as it was about to fail (it needed to be replaced with a new one just after this campaign).

2. Autofocus approaches adapted

The two autofocus methods that can be either be directly used or improved to deal with 2D aperture autofocus are both based on the frame drift approach (measure of the mismatch between detected images from two separate sub-apertures), assuming the mismatch is space varying (hence, measuring mismatch on small sub-images in the whole scene) and trying to update the trajectory (i. e. the autofocus produces an updated trajectory, and not a sharpened image. In both cases, the updated trajectory can be used to re-synthesise a sharper SAR image or to refocus the SAR image by local space varying convolution).

The first and older method can be directly applied to the present problem. Its principle is to define a grid of small sub-images (possibly overlapping) on one master image and map the sub-image centres to one (or several) slave(s) image(s). The slave sub-image around each sub-image sub-image centre is mapped to the master sub-image geometry using a linear transformation (using a geometrical model of the sensor). The distortion from the master sub-image to the mapped slave sub-image is close to a mere translation that can be estimated by correlating the two images and locating the maximum.

Then a slave trajectory distortion is estimated by minimising the difference between the estimated and modelled image distortion. (In fact the shapes of the correlation maxima are used to weight the translation measure, thus allowing for example matching a linear feature in which case only one degree of freedom is constrained see [1] for the original method designed for front looking IR sensor & [2] for details on the SAR usage). The trajectory distortion model can be common to both images (e.g. for autofocus using two looks from the same acquisition) or apply only on the slave (e.g. for repeat-pass interferometry, see [3] for an old example).

The second method is the autofocus currently in use at ONERA. Unlike the older method, it generates the sub-images on the fly thus allowing a coarse to fine resolution approach and yield trajectory updates for higher distortion frequencies. In order to efficiently compute the sub-images, a strongly down-sampled signal clipped to a range interval and Doppler filtered to a neighbourhood of the sub-image centre is first generated, and fast polar format algorithm is used for synthesis. See [4] for details.

However, as such the autofocus program was designed only for focusing a single monostatic or bistatic SAR image and can not accommodate images from several acquisitions (nor of course optical images). It is used for focusing the master image (Fig. 3), but for matching (and by the way focusing) slave images it needed to be modified:

First, the correlated sub-images instead of being synthesised from the same (down-sampled & filtered) signal for successive apertures, are synthesised from two signals (from both acquisitions) for matching apertures (with trajectory update only on the slave signal).

Second, the update to mismatch relation (to be inverted for improving the update) must be modified for accounting that only the slave image is affected (note that the system becomes more sensitive because the position is directly involved instead of the velocity).

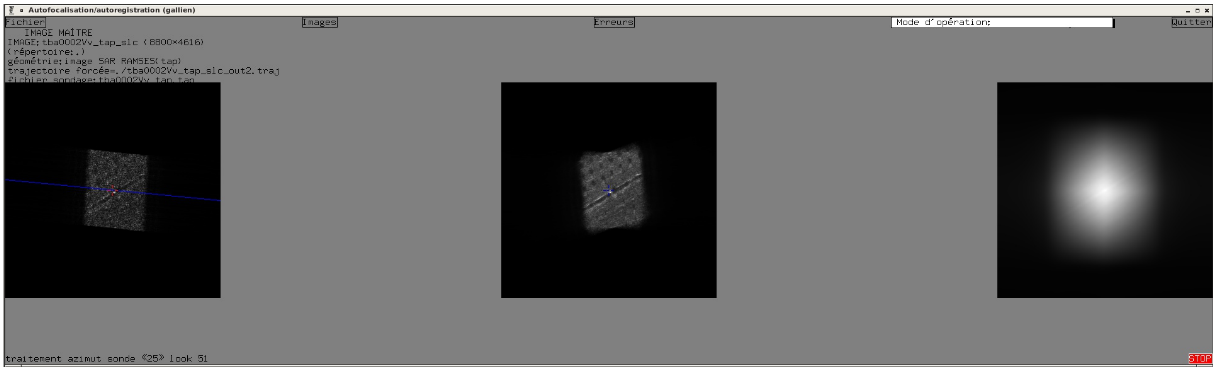

Figure 3: Illustration of the autofocus process for the master image (flight 0, take 2). It is a “debug mode” screen capture during the third pass (still at low resolution) with a single look sub-image synthesised from the twice updated trajectory (left) on which the azimuth axis is the blue line, the multi-look image from the previous apertures registered (centre) on which the successive sub-image centres are plotted in blue, and the correlation between the single look and multi-look sub-images (right) which determines the translation to be applied to the single look before adding it to the multi-look.

One important point for the registration of the 17 slaves acquisition lines is that the sub-images must have a defined altitude, i. e. the corresponding areas must correspond to surface echo area and not volume echo area (and this is even more mandatory for the next section). In order to select the appropriate landmarks, we used a mask build from the coherency of the single pass Vv polar interferogram obtained from the Vv channel of the master image (flight 0, take 2, right pod) and the bistatic right pod to left pod Vv image (Fig. 4).

Figure 4: Correlation of the single pass Vv interferogram used for landmark selection for master autofocus & slaves registration. White (coherence close to one) area corresponds to surface echoes, dark (coherence close to zero) areas correspond to volume echo areas (forest, urban), low backscatter (channel, river & lake) and cast shadows. Horizontal dashed line on the right is a power cable (makes the echo in volume because the cable is 10 m above ground), short oblique stripes on the airfield are de-localised/defocused truck running the highway at the centre.

The first (older) autofocus method needed also an improvement for this problem: The sub-images are taken in a rectangular grid, but there is no provision to discard the sub-images that are in the masked (volume echo) area. Indeed, the measured mismatches are weighted in function of the sharpness of the correlation peak (and the peak is twice sharper in one-coherence area than is is in zero-coherence area) but incorporating an external mask would be more efficient.

3. Further registration

The master image is further registered (less than 4 m trajectory offset) using the geodetic point images (it is not an absolute requirement but it allows having directly the resulting images in accurate ground coordinates).
Slave image trajectories are registered with respect to the master trajectory with an accuracy of a fraction of the range resolution (for the cross-track direction) and the sub-aperture maximum azimuth resolution (for the along-track direction) which are respectively 30 cm and 10 cm. This accuracy is approximately one order of magnitude lower than the requirement for the 2D aperture focusing.
In case the imaged landscape is mostly with surface echoes (as this is obviously the case for our dataset) it would be possible to unwrap the phase of the interferogram after registration and use the classical “orbital fringe removal” approach to remove the remaining slave trajectory error (i. e. a baseline bias). But in the case of mostly forested area, the unmasked “surface echo” area would not be connected and the phase unwrapping would not be possible.
However, it is still possible that the slave image registration could be possible -in the coherent area- with an accuracy with is a fraction of the resolution of the order of the relative bandwidth (5% in our dataset). This is plausible, since the correlation peak in the one-coherence case has the shape of the squared pulse response (square of the image of a perfect isotropic white reflector), thus the image resolution correspond to slightly more than the 6 dB width of the correlation peak. If it is the case, the multilateration could be continued with the phase difference between the master and slave sub-images (and not the translation between them), and the relative position of the slave trajectory could be updated beyond the required accuracy for 2D aperture focusing.

Figure 5: Interferogram of the Vv channel between the bistatic image (transmitted from right wing antenna & received from left wing antenna) and the monostatic image (transmitted & received from right wind antenna) during flight 0 take 2. Note that this is compensated by the DTM (DTED level 1) which tends to smooth the narrow ridges around the small river, and of course completely ignores the highway ridge through the hill between the airfield and the town.

Figure 6: Interferogram of the Vv channels between the monostatic images (transmitted & received from right wind antenna) during flight 0 take 3 and take 2 (also DTM compensated) after registration by the older autofocus algorithm (without the proposed masked area improvement). Note that the baseline is much higher than in the previous interferogram (from about 20 m at the beginning to 53 m at the end of the take compared to the 4 m baseline = half the separation between left wing & right wing antennae). Note also the higher coherency loss in the town and the golf course on the right side.

4. Limitation & further work

The approach requires that at any position during the acquisition flat surface echo areas are within the antenna pattern in at least three non aligned directions (in order to obtain a full 3D

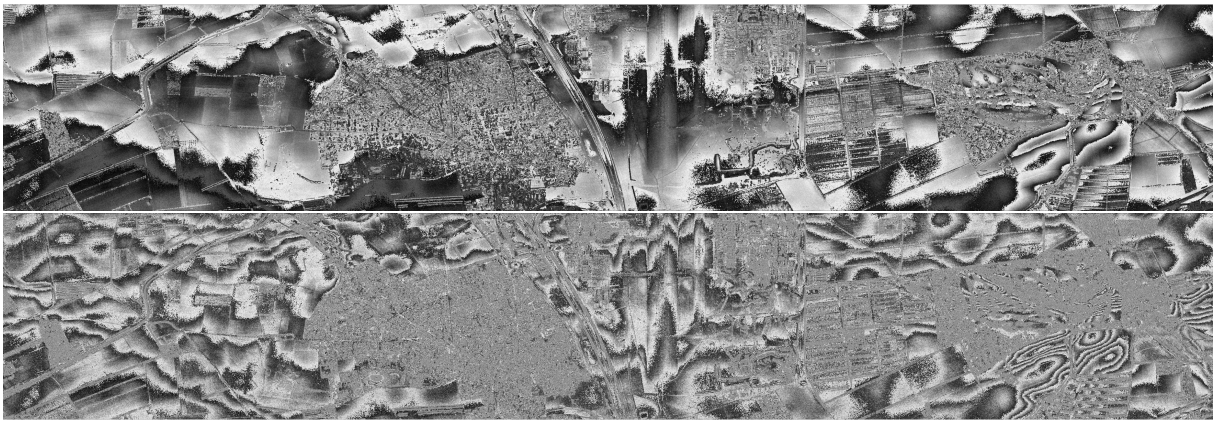

Figure 7: Interferogram from fig. 5 with phase multiplied by 5.4 (top) and 14 (bottom). The left part of the top image should look like the left part of fig. 6 while the right part of bottom image should look like the right part of fig. 6. Of course the phase detail is not exact because the baseline between take 3 and take 2 is not exactly horizontal!

trajectory update). This is obviously the case in our dataset (Fig. 4) but this may be problematic for acquisitions in fully forested areas (such as Amazonian forest) and would constraint the image footprint to contain some dispersed deforested (urban, industrial or agricultural) area.
This work is still in progress, the two above described improvements of the autofocus (namely using a reference sub-image from the master acquisition and switching to sub-image phase difference after the coarse to fine stages) are under way, and three-dimensional full polar tomographic images are not yet obtained, result should be shown in the final paper print.

Acknowledgements

This project has been funded by ANR (the French National Research Agency) and DGA (Direction Générale de l'Armement) under ALYS project ANR-15-ASTR-0002.

References

[1] M.L. Duplaquet, H. Cantalloube "Une méthode globale de recalage inter-images", *Proc. of 1993 GRETSI colloquium*, Juan les Pins, France, 1993, pp. 885-888.

[2] H. M-J. Cantalloube C.E. Nahum "Autofocusing of (inverse) synthetic aperture radar for motion compensation", *Proc. of IEEE National Aerospace & Electronics Conf.*, Dayton OH, USA, 20-23 may 1996, vol.1 pp. 309-316.

[3] H. M-J. Cantalloube C.E. Nahum "Repeat-Pass airborne SAR interferometry", *Proc. of EUSAR Conf.*, Munich, Germany, 23-25 may 2000, pp. 489-492

[4] H. M-J. Cantalloube C.E. Nahum "Multiscale Local Map-Drift-Driven Multilateration SAR Autofocus Using Fast Polar Format Image Synthesis", *IEEE Trans. on Geoscience and Remote Sensing*, Oct 2011, vol. 49, no. 10 part 1, pp. 3730-3736.